International Journal of Heat and Mass Transfer 52 (2009) 1431–1442

Contents lists available at ScienceDirect

International Journal of Heat and Mass Transfer

journal homepage: www.elsevier.com/locate/ijhmt

On the applicability of the heat and mass transfer analogy in indoor air flows

H.-J. Steeman [a,*], A. Janssens [b], M. De Paepe [a]

[a] Department of Flow, Heat and Combustion Mechanics, Ghent University – UGent, Sint-Pietersnieuwstraat 41, 9000 Gent, Belgium
[b] Department of Architecture and Urbanism, Ghent University – UGent, Jozef Plateaustraat 22, 9000 Gent, Belgium

ARTICLE INFO

Article history:
Received 3 March 2008
Received in revised form 4 August 2008
Available online 22 October 2008

Keywords:
Heat and mass transfer analogy
Indoor air
Heat and moisture transfer
CFD

ABSTRACT

The heat and mass transfer analogy is used in building simulation to convert heat transfer coefficients into mass transfer coefficients. The analogy is valid under strict conditions. In this paper CFD is used to investigate the accuracy of the analogy for indoor air flows when not all these conditions are met. CFD simulations confirm the possibility of applying the analogy to indoor air flows and show that when not all conditions are met, the average mass transfer coefficients remain well predicted by the analogy while the prediction of local transfer coefficients can result in large errors.

1. Introduction

In the design stage of a building it is important that a proper assessment can be made of the relative humidity inside the building. The indoor relative humidity should be kept within a given range to assure the comfort of the occupants and to prevent deterioration of building materials and objects (e.g. artefacts in museums). In both cases moisture exchange between the indoor air and porous materials inside the building plays an important role.

When the interest lies in predicting Indoor Air Quality (IAQ) the moisture exchange with the walls is important as it is part of the transient water vapour balance of a room which determines the average indoor relative humidity [1]. For this type of problems multi-zonal models are used to predict the average indoor relative humidity and temperature [1–3]. Such models use an average water vapour transfer coefficient to calculate the moisture flux to the different moisture buffering walls. As little direct experimental data is available on water vapour transfer coefficients the heat and mass transfer analogy is used to calculate them [4].

If the risk of moisture related damage in a building is to be assessed then the interest of the study lies in the hygrothermal behaviour of materials rather than in the average humidity of the indoor air. In this case local surface transfer coefficients are required to describe the interaction of individual objects with the indoor air. Local heat transfer coefficients can be measured, yet it is extremely difficult to experimentally obtain local water vapour transfer coefficients on site. It might thus be useful if the heat and mass transfer analogy could be applied to calculate local transfer coefficients. An example of a study where the analogy was used to calculate local mass transfer coefficients can be found in [5].

Despite the frequent use of the heat and mass transfer analogy, it is not clear how well the analogy actually performs inside buildings. The heat and mass transfer analogy was originally developed for forced boundary layer flow over flat plates or inside tubes [6] while in buildings a natural or mixed convection flow occurs over a sometimes complex geometry. Secondly the presence of heat and moisture sources and the different boundary conditions for heat and moisture transport at the wall surfaces in practical cases make it quasi impossible to fulfil the conditions under witch the analogy is valid. Hence the aim of this paper is twofold: first we want to check the validity of the analogy in indoor air flows and secondly we want to investigate how strong the accuracy of the analogy deteriorates for the different flow regimes encountered inside buildings in case not all limiting conditions are fulfilled.

As the experimental validation of the analogy in buildings is extremely difficult Computational Fluid Dynamics (CFD) is used in this paper to carry out the study on the heat and mass transfer analogy. Using CFD heat, air and moisture transport in a room can be simulated with perfect control of all boundary conditions and with perfect knowledge of the results. The drawback of CFD is that simulation results of turbulent flow have to be treated with caution: the turbulence models employed in CFD are not universally applicable and for some specific situations none of the known turbulence models results in accurate predictions. Special attention was hence paid in this paper when selecting the turbulence model.

In the course of time different formulations of the heat and mass transfer analogy have been proposed. Before testing the

* Corresponding author. Tel.:+32 9 264 3289; fax: +32 9 264 3575.
E-mail address: hendrikjan.steeman@ugent.be (H.-J. Steeman).

0017-9310/$ - see front matter © 2008 Elsevier Ltd. All rights reserved.
doi:10.1016/j.ijheatmasstransfer.2008.09.006

Nomenclature

A	wall surface area (m^2)
c	concentration (kg/m^3)
C_f	skin friction coefficient
Cp	heat capacity (J/kgK)
D	mass diffusivity (m^2/s)
g	acceleration of gravity (m^2/s)
G	moisture flux (kg/m^2s)
Gr	Grashof number, $Gr = g(\rho_{right}-\rho_{left})L^3\rho/\mu^2$
h	heat transfer coefficient (W/m^2K)
j	j factor from Chilton–Colburn
L	characteristic length (m)
Le	Lewis number, $Le = Sc/Pr$
M	molar mass (g/mol)
$MTCR$	ratio of predicted and simulated mass transfer coefficients
Nu	Nusselt number, $Nu = hL/\lambda$
Pr	Prandtl number, $Pr = \mu/\rho\alpha$
Q	heat flux (W/m^2)
Re	Reynolds number, $Re = \rho vL/\mu$
Ri	Richardson number, $Ri = Gr/Re^2$
Sc	Schmidt number, $Sc = \mu/\rho D$
St	Stanton number, $St = Nu/RePr$ or $St = Nu/ReSc$
t	time (s)
T	temperature (K)
v	velocity (m/s)
V_0	buoyancy velocity, $V_0 = \sqrt{g\beta\Delta\rho L/\rho}$ (m/s)
x	coordinate along width of cavity
y	coordinate along height of cavity
Y	dimensionless height $Y = y/L$

Greek symbols

α	thermal diffusivity (m^2/s)
λ	thermal conductivity (W/mK)
μ	dynamic viscosity (kg/ms)
θ	dimensionless temperature (-)
ρ	density (kg/m^3)
$\bar{\omega}$	dimensionless species mass fraction (-)
ω	species mass fraction / Specific humidity (kg/kg)

Subscripts

H	heat transfer
m	mass transfer
ref	reference
S	surface
∞	free stream

Superscripts

c	concentration
ω	species mass fraction

accuracy in indoor air flows an overview is given of the different analogies, their limiting conditions and applicability.

2. Heat and mass transfer analogy

2.1. Available analogies

Reynolds was the first to report on the analogous behaviour of heat and momentum transfer. He presented results on frictional resistance to fluid flow in conduits which made the quantitative analogy between the two transport phenomena possible. Out of these observations the Reynolds analogy was stated [7]. The Reynolds analogy relates the heat transfer coefficient (h) to the skin friction coefficient (C_f) using the free stream velocity (v_∞) and the free stream density (ρ) and heat capacity (Cp):

$$St = \frac{h}{\rho v_\infty C_p} = \frac{C_f}{2} \tag{1}$$

This relation can be deduced out of the boundary layer equations for laminar forced flow over a solid surface under the conditions that the Prandtl number (Pr) is equal to one and no form drag is present. The Reynolds analogy can also be applied to mass transfer in case the Schmidt number (Sc) is equal to one:

$$St_m = \frac{h_m^c}{v_\infty} = \frac{C_f}{2} \tag{2}$$

with h_m^c the mass transfer coefficient with species concentrations as driving force. In case both Pr and Sc numbers are equal to one, and hence the Lewis number (Le) is one, Eqs. (1) and (2) can be combined to a relation between the mass transfer coefficient and the heat transfer coefficient:

$$\frac{St}{St_m} = \frac{h}{\rho C_p h_m^c} = 1 \tag{3}$$

The Reynolds analogy is limited in its application because of the strict conditions under which it is valid. Yet this analogy inspired researchers to seek for analogies which are more generally applicable. Prandtl developed an analogy for heat and momentum transfer and for mass and momentum transfer considering the turbulent core and the laminar sublayer in the boundary layer equations [7]. The effect of Pr and Sc numbers different from one is taken into account in this analogy. This led to the following equations for the heat and mass transfer coefficients:

$$St = \frac{h}{\rho C_p v_\infty} = \frac{C_f/2}{1 + 5\sqrt{C_f/2}(\mathrm{Pr} - 1)} \tag{4}$$

$$St_m = \frac{C_f/2}{1 + 5\sqrt{C_f/2}(Sc - 1)} \tag{5}$$

von Karman extended Prandtl's work and took the effect of the transition layer between the laminar sublayer and the turbulent core into account [7]. This led to an extra correction term as function of respectively Pr and Sc in Eqs. (4) and (5). The application of the Prandtl and von Karman analogies is restricted to cases with negligible form drag. Both the Prandtl analogy as the von Karman analogy reduce to the Reynolds analogy for Pr and Sc number equal to one.

While Prandtl and von Karman adapted the Reynolds analogy by considering the transfer equations in the boundary layer, Chilton and Colburn sought modifications to the Reynolds analogy using experimental data [6,8]. They suggested a simple modification for situations with Pr and Sc numbers different from unity. This was done by defining the j factor for heat transfer and the j factor for mass transfer:

$$j_H = StPr^{2/3} = C_f/2 \tag{6}$$

$$j_m = St_m Sc^{2/3} = C_f/2 \tag{7}$$

Colburn applied the j factor for heat transfer to a wide range of data for flow on different geometries and found it to be quite accurate for conditions where no form drag exists and for Pr between 0.5 and 50. The complete Chilton–Colburn analogy is found when Eqs. (6) and (7) are combined:

$$\frac{St}{St_\mathrm{m}} = \frac{h}{\rho C_\mathrm{p} h_\mathrm{m}^\mathrm{c}} = Le^{2/3} \tag{8}$$

When form drag is present neither j_H or j_m equals $C_\mathrm{f}/2$, yet it has been shown that Eq. (8) remains valid [9]. It is clear that the Chilton–Colburn analogy also reduces to the Reynolds analogy for Pr and Sc numbers equal to unity. Unlike the Prandtl or von Karman analogy the relation between the heat and mass transfer coefficients is no longer function of the skin friction coefficient.

The analogy between heat and mass transfer is expressed by the ratio of St and St_m. This ratio is called the Lewis factor or Lewis relation and should not be confused with the Lewis number. Depending on the use of either the Reynolds analogy or the Chilton–Colburn analogy the Lewis relation becomes either unity or $Le^{2/3}$. These two Lewis factors are generally used when relating heat and mass transfer.

The analogy between heat and momentum transfer and between mass and momentum transfer is based on the assumption that respectively the dimensionless velocity and temperature profiles and the dimensionless velocity and species concentration profiles are similar. This is the case for forced convection flow over a solid surface without form drag. All the analogies mentioned in this paragraph were developed for this case.

2.2. Natural and mixed convection

Inside buildings temperature differences generate buoyancy forces which cause air movement. The flow inside buildings is thus driven by natural convection or by mixed convection. In case of natural and mixed convection the dimensionless velocity profile is no longer similar to the dimensionless temperature or species concentration profile due to the presence of the buoyancy force which adds and extra source term in the momentum equation. The analogy between momentum transfer and heat or mass transfer is lost. The question which is raised now is whether the analogy between heat and mass transfer is still valid for these situations and if so, under which conditions? To answer these questions the transport equations for heat and mass transfer in fluids are studied:

$$\rho C_\mathrm{p} \frac{DT}{Dt} = \rho C_\mathrm{p}\left(\frac{\partial T}{\partial t} + \vec{v}.\nabla(T)\right) = \nabla(\rho \alpha C_\mathrm{p} \nabla T) \tag{9}$$

$$\rho \frac{D\omega}{Dt} = \rho\left(\frac{\partial \omega}{\partial t} + \vec{v}.\nabla(\omega)\right) = \nabla(\rho D \nabla \omega) \tag{10}$$

$\vec{v}$ represents the velocity vector, α the thermal diffusivity, ω the mass fraction of the transported species and D the diffusivity of the transported species. In case of water vapour transfer in air the species mass fraction ω is also called specific humidity. Eqs. (9) and (10) are valid for isobaric compressible and incompressible flow without heat or mass sources and with negligible viscous dissipation. Mass transport is assumed to take place in a dilute gas. If this assumption is not fulfilled the diffusion term in Eq. (10) becomes a function of all species gradients and the analogy with heat transfer is lost. In case of simultaneous heat and mass transport an extra term has to be added to the heat transfer equation representing the energy transported with the mass diffusion. Bottemanne showed that if the partial pressure of the transported species is much smaller than the total pressure (as in the case of water vapour transport in air) the mutual influence of heat and mass transport can be neglected [10]. Hence Eqs. (9) and (10) also approximate simultaneous heat and moisture transport in air. No assumptions are made in these equations on the velocity or the thermal and mass diffusivity. It is assumed that for small density variations, as encountered in buildings, the incompressible formulation (Eqs. (9), (10)) can be used. These equations are valid for as well forced convection as for natural convection in buildings. The use of the analogy between heat and mass transfer in buildings is only allowed if Eqs. (9) and (10) are of similar shape and if the density and velocity field are the same in both transport equations.

In case of forced convection heat and moisture transfer the velocity field is fully determined by the momentum boundary conditions and the variations in density are usually small enough to be neglected. Hence the condition that the velocity field and the density field should be identical is easily fulfilled. A characteristic feature of natural convection is the varying density which causes the buoyant force and determines the velocity field. Hence the density cannot assumed to be constant and the velocity field is no longer independent of the heat and mass boundary conditions. To assure an identical velocity and density field the heat and mass transport should occur simultaneously. According to Beddingfield the different effect of temperature and humidity on density and viscosity is not that important that the analogy is lost in humid air [11]. This means that in case of a similar velocity field the analogy applies for separate heat and moisture transport in air.

If the analogous behaviour of Eqs. (9) and (10) is used to derive the Reynolds analogy, then the following relations are obtained:

$$\frac{h}{C_\mathrm{p}} = \frac{Q}{C_\mathrm{p}(T_\mathrm{s} - T_\mathrm{ref})} = \frac{\rho \alpha C_\mathrm{p} \nabla T_\mathrm{s}}{C_\mathrm{p}(T_\mathrm{s} - T_\mathrm{ref})} = \frac{\rho \alpha \nabla T_\mathrm{s}}{(T_\mathrm{s} - T_\mathrm{ref})} \tag{11}$$

$$h_\mathrm{m}^\omega = \frac{G}{(\omega_\mathrm{s} - \omega_\mathrm{ref})} = \frac{\rho D \nabla \omega_\mathrm{s}}{(\omega_\mathrm{s} - \omega_\mathrm{ref})} \tag{12}$$

Note that the mass transfer coefficient is now written for species mass fractions as driving force. If the Lewis number is one α equals D and Eqs. (11) and (12) yield equal right hand sides when written in function of dimensionless temperatures and species mass fractions. The following relation is found:

$$\frac{h}{C_\mathrm{p}} = h_\mathrm{m}^\omega \tag{13}$$

Comparison of Eqs. (3) and (13) shows that the latter equation reduces to the first if the density is constant. In that case the difference in species concentration equals the density multiplied with the difference in species mass fraction. Hence Eq. (13) is a more general representation of the Reynolds analogy. As the Reynolds analogy is valid for natural convection it is expected that the Chilton–Colburn analogy expressed as function of h_m^ω will also yield good results.

The choice of the reference condition in Eqs. ((11), (12)) is less straightforward for natural convection in an enclosure than for forced convection over a flat plate. In case of forced convection the free stream conditions can be used as a reference, yet for natural convection no real free stream can be defined. Different authors have made different choices for the reference condition in an enclosure. Two categories of references can be distinguished: a single reference for all the walls of the enclosure and different references for different points on the walls. Examples of single reference choices are the average condition in the air volume [12] and the condition at the centre of the air volume [13]. An example of the second category of references is the choice of the conditions outside the boundary layer at 10 cm from the wall surface [13].

In the previous part of the paper the analogy between heat and mass transfer was assumed to be valid if the transport equations are of similar form. It is evident that also the boundary conditions have to be similar for the analogy to be directly applicable. This conclusion was also drawn by Masmoudi in a study about forced convection drying of a capillary porous material [14].

3. Methodology for assessing the heat and mass transfer analogy

3.1. General

Using CFD the transport equations for momentum, heat and mass transfer in fluids are numerically solved which results in simulated velocity, temperature and species concentration fields and allows for the calculation of heat and mass fluxes. The species of interest in this paper is water vapour and the studied flow is natural and mixed convection in an enclosure. The choice is made to model the indoor air in the enclosure using the temperature and specific humidity at the wall surfaces as boundary conditions. The transport phenomena inside the porous walls are not considered. In the search for the limits of the heat and mass transfer analogy simulations with extreme differences in temperature and humidity conditions at the walls will be performed. These extreme boundary conditions represent worst case scenarios for the use of the analogy in practical cases (i.e. in building simulation).

CFD yields both heat and mass transfer coefficients. The CFD generated heat transfer coefficients can be used as input for the heat and mass transfer analogy to predict the mass transfer coefficients. Taking the ratio of the predicted and the directly calculated mass transfer coefficient makes it possible to judge the performance of the analogy and to describe it with one single number. This ratio is called the mass transfer coefficient ratio (MTCR) and should ideally be one. Deviations from one represent over or under predictions of the mass flux to the walls. The MTCR can be calculated for as well local mass transfer coefficients as for average transfer coefficients. The equations for the local and average MTCR are respectively given in Eqs. (14) and (15) for the Chilton–Colburn analogy. Mass averaged indoor conditions are used as reference condition.

$$\text{local\_MTCR} = \frac{\frac{h}{Le^{2/3}C_p}}{h_m^{\omega}} \tag{14}$$

$$\text{average\_MTCR} = \frac{\int_S h(T_s - T_{ref})\mathrm{d}A}{\int_S T_s \mathrm{d}A - T_{ref}A} \frac{1}{Le^{2/3}C_p} \frac{\int_S \omega_s \mathrm{d}A - \omega_{ref}A}{\int_S h_m^{\omega}(\omega_s - \omega_{ref})\mathrm{d}A} \tag{15}$$

The flow inside a building can be considered as natural, forced or mixed convection depending on the driving force. In the first case the flow is entirely driven by buoyancy, in the second case the flow is driven by air movement caused by a fan or by external pressure differences and in the last case a combination of both driving forces is present. These different flow regimes can be characterized by a single dimensionless number, i.e. the Richardson number. This number gives the ratio of the buoyancy and the inertial forces and is defined as:

$$Ri = \frac{Gr}{Re^2} = \frac{g\frac{\Delta\rho}{\rho}L}{v^2} \tag{16}$$

In this paper simulations will be performed for Ri numbers equal to infinity (natural convection), 10 (dominating natural convection), 1 (perfect mixed convection) and 0.1 (dominating forced convection), representing all the relevant flow regimes inside buildings. The performance of the heat and mass transfer analogy will be tested for different scenarios under these four flow regimes. To limit the computational cost only 2D cases are considered.

3.2. Description of the studied cases

The different scenarios simulated in this paper are based on the same case. This base case is a 2D simultaneous heat and moisture transfer problem in a rectangular room with dimensions of 2.5 × 2.5 m (Fig. 1.). The floor and ceiling of the room are adiabatic and impermeable to water vapour. At the two vertical walls constant temperatures and specific humidity are imposed (20 °C and 7.21 g/kg at the left wall and 30 °C and 13.1 g/kg at the right wall corresponding with a relative humidity of 50% at each wall). The temperature is made dimensionless using the following equation:

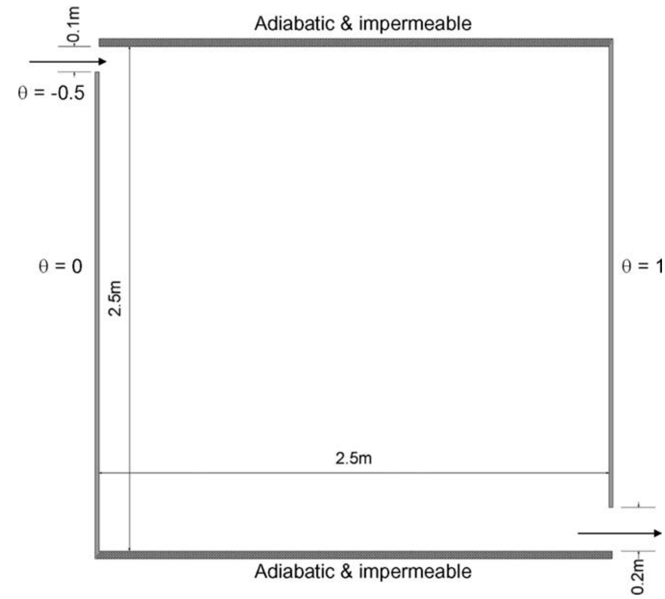

Fig. 1. Geometry of the studied enclosure with dimensionless boundary conditions for the base case.

$$\theta = \frac{T - T_{s,left}}{T_{s,right} - T_{s,left}} \tag{17}$$

If a similar equation is used for the specific humidity then the base case can be characterized by a dimensionless temperature and specific humidity of zero at the left wall and one at the right wall.

A constant velocity inlet with a height of 0.1 m is situated at the top of the left wall while an outlet with a height of 0.2 m is situated at the bottom of the right wall. The velocity profile at the inlet is fully developed with a maximum velocity set by the Ri number (Eq. (16)). The turbulence at the inlet is characterized by a turbulence intensity of 10% and a turbulence length scale of 0.007 m. The dimensionless temperature and specific humidity at the inlet are both −0.5 which corresponds with 15 °C and 4.25 g/kg and assures the analogy of the boundary conditions. The Rayleigh number characterising the base case is 1.75E10 for Ri equal to one. This indicates that the flow in the room is fully turbulent.

Table 1 describes the changes made to the base case which will be used as alternative scenarios. Analysis of the transport equations showed that the heat and mass transfer analogy could be used to relate individual heat and mass transfer problems with equal Pr and Sc number (thus $Le = 1$) in case of analogous boundary conditions and identical velocity and density fields. In applications like building simulation the analogy is however used to relate simultaneous heat and mass transport with different Pr and Sc numbers and non-analogous boundary conditions. Different scenarios are simulated to investigate the effect of Lewis number (Base case, Lewis1), simultaneous or separate transport (Base case, Separate, Equal Gr), moisture sources (Uniform Source, Discrete Source) and non-analogous boundary conditions at the walls (Diff-BC1-3). For the natural convection cases no air is introduced in the enclosure and the inlet and outlet sections of the computational

Table 1
Description of the different scenarios used to evaluate the heat and mass transfer analogy

Scenario	Description
Base case	Simultaneous heat and moisture transfer with $Pr = 0.75$ and $Sc = 0.58$
Lewis 1	Simultaneous heat and moisture transfer with $Sc = Pr = 0.75$
Separate	Separate heat and moisture transfer with $Sc = Pr = 0.75$
Equal *Gr*	Separate heat and moisture transfer with $Sc = Pr = 0.75$. Temperature difference reduced: $Gr_H = Gr_m$
Uniform source	Base case + Uniform water vapour source in entire indoor volume: 0.02 kg/m^{3}h
Discrete source	Base case + Water vapour source in one quarter of the indoor volume located at the left bottom: 0.08 kg/m^{3}h
DiffBC1	Base case + Linear moisture concentration profile at the left wall: 7.21 g/kg at $y = 0$ m and 13.1 g/kg at $y = 2.4$ m
DiffBC2	Base case + Linear moisture concentration profile at the right wall: 7.21 g/kg at $y = 2.5$ m and 13.1 g/kg at $y = 0.2$ m
DiffBC3	Base case + Discrete moisture concentration profile at the right wall: 26.5 g/kg at $y < 0.7$ m and 7.21 g/kg at $y >= 0.7$ m

domain are treated as walls. The boundary conditions for these new walls are the same as for the adjacent vertical walls (in case of linear profiles the profile is stretched to include the new wall).

3.3. CFD settings

As the CFD simulations will be used to check the accuracy of the heat and mass transfer analogy it is important that the fluid properties are correctly represented in the CFD model. Earlier in the paper it was stated that the incompressible formulation of the transport equations could be used inside buildings. For this reason the incompressible ideal gas relation is used to model the varying density. Unlike the boussinesq model the incompressible ideal gas relation takes both the effect of temperature and species concentration into account. Other relations used to model fluid properties include the mass weighted mixing law for the determination of the heat capacity and the ideal gas mixing law for the calculation of the thermal conductivity and the dynamic viscosity. The heat capacity, thermal conductivity, dynamic viscosity and molecular weight of the different species (air and water vapour) and the mass diffusivity of water vapour in air are assumed to be constant and are given in Table 2. This assumption was checked by comparing the simulated specific humidity for CFD simulations with varying and with constant fluid properties. A maximum difference of 1.5% was found.

A second order upwind scheme is used for the discretization of the convective terms in the transport equations in order to reduce numerical diffusion. The PRESTO! scheme is used for the discretization of the pressure. The SIMPLE algorithm is used for the pressure–velocity coupling. A double precision representation of real numbers is used to reduce round-off errors.

As the interest of the study lies in the heat and mass fluxes to the walls it is important that the near wall behaviour of the flow is correctly represented. A sufficiently refined grid is used near the wall (y+ <4) in combination with a low-Reynolds-number k-ω turbulence model. This turbulence model is known to perform very well close to walls. Unlike wall functions, which impose a known velocity profile near the walls, the k-ω model can be used to actually simulate the flow close to the walls and is applicable for as well natural as forced convection.

3.4. Validation

To validate the used settings a 2D natural convection experiment for the validation of CFD codes is simulated [15]. The validation experiment is very similar to the natural convection cases simulated in this paper except that the height and the width of the experimental chamber are only 0.75 m and the temperature difference between the hot and cold wall is 40 K instead of 10 K. The Rayleigh number for the experiment is 1.58E9. Because of the similarities between the experiment and the studied cases the experiment is considered a representative validation case.

First the grid sensitivity of the simulation is studied by refining the computational grid with a factor 2 and with a factor 4 in all dimensions and checking the effect on the heat flow through the hot wall. The original grid is a structured grid counting 12862 rectangular cells. The grid is dense near the walls and gradually coarsens towards the centre of the room. The heat flow entering the room through the hot wall is 54.56 W for the original grid and changes to respectively 54.96 W and 55.24 W for the refined grids. Hence it can be concluded that the original grid produces results which are accurate (deviation between subsequent grid refinements smaller than 1%) but not grid independent. Given the large number of cases to be simulated and the high computational cost to reach grid independent solutions the original grid was retained.

Secondly the simulated and experimentally obtained temperature and velocity profiles at $Y = 0.5$ near the hot wall are compared in Fig. 2. This figure shows that the agreement between experiment and simulation is rather good. In the last part of the validation the local Nusselt number at the hot wall is considered. Fig. 3. shows that Nusselt number is accurately predicted for the largest part of the wall, yet for the bottom part the experiment and simulation do not coincide. However, comparison between this numerical study and a numerical study by Beghein [16] shows a very good agreement even for the bottom part of the wall. This indicates that the CFD settings and the computational grid described in this chapter are suited for the simulation of indoor flow driven by buoyancy forces.

4. Results

The results of the CFD analysis for the different scenarios and flow regimes described in the previous chapter are given in Tables 3 and 4, and Figs. 4 and 5. In Figs. 4 and 5. the local MTCR is plotted while in Tables 3 and 4 the average MTCR is given. The MTCR is calculated with the Chilton-Colburn analogy using the mass averaged indoor conditions as a reference (Table 3, Figs. 4 and 5.) or using the inlet conditions as a reference (Table 4). For the base case the average MTCR is also calculated using the Reynolds analogy and the mass averaged indoor conditions as reference (Table 3).

4.1. Natural and mixed convection

When the average MTCR calculated with the Chilton–Colburn analogy and the Reynolds analogy are compared for the base case, it can be noticed that the Chilton–Colburn analogy gives superior results. The deviations found between the average mass transfer coefficient predicted with the Chilton–Colburn analogy and the

Table 2
Fluid properties used in the CFD simulations

Property	Air	Water vapour
C_p/(Jkg^{-1}K^{-1})	1006.43	1905.9
λ/(Wm^{-1}K^{-1})	0.0242	0.01823
μ/(kgm^{-1}s^{-1})	1.7894 E-5	9.727 E-6
M/(gmol^{-1})	28.966	18.01534
D/(m^{2}s^{-1})	2.55 E-5	

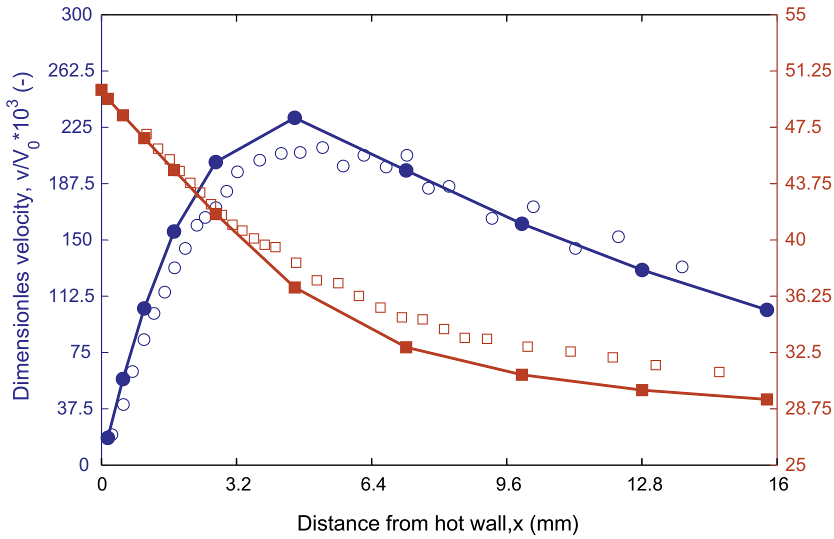

Fig. 2. Comparison between a natural convection validation experiment [15] and the CFD simulation for temperature and velocity profiles at $Y = 0.5$ with (–■–) the simulated temperature, (□) the measured temperature, (–●–) the simulated velocity and (○) the measured temperature.

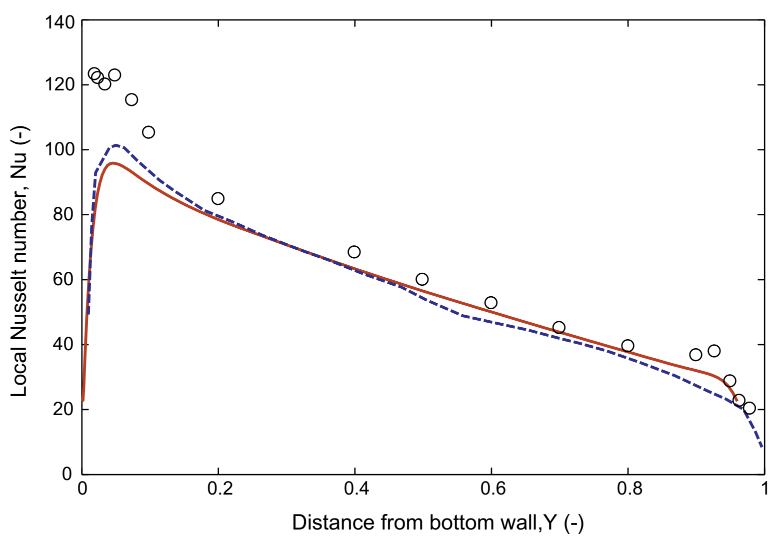

Fig. 3. Comparison between the local Nusselt numbers at the hot surface of the enclosure obtained from a validation experiment (○), an existing CFD study [16] (–) and the new CFD study (-----).

Table 3

Average MTCR for the left and right wall using the mass averaged indoor conditions as a reference for the Chilton–Colburn analogy (CC) and the Reynolds analogy (*Re*)

Scenario	*Ri* 0.1		*Ri* 1		*Ri* 10		Natural convection	
	Left	Right	Left	Right	Left	Right	Left	Right
Base case (CC)	0.993	0.999	0.987	0.992	-0.058	0.984	0.995	1.008
Base case (Re)	0.834	0.839	0.83	0.835	-0.049	0.834	0.854	0.864
Lewis 1 (CC)	1.017	1.031	0.999	1.018	1.09	1.022	0.993	1.006
Separate (CC)	1.014	1.012	1.08	1.093	4.134	1.697	1.809	1.799
Equal *Gr* (CC)	0.994	0.996	0.98	0.984	0.968	0.985	0.997	0.998
Uniform source (CC)	0.956	0.973	0.957	0.948	-5.501	0.96	1.124	-0.294
Discrete source (CC)	0.993	0.976	1.027	0.929	-5.056	0.974	1.404	8.642
DiffBC1 (CC)	0.995	0.985	0.996	0.978	3.376	0.983	0.593	0.892
DiffBC2 (CC)	0.998	0.97	1.003	0.996	2.589	1.051	1.179	1.519
DiffBC3 (CC)	0.984	0.925	0.993	1.006	1.69	1.027	1.285	2.314

directly simulated average mass transfer coefficient are smaller than 2% except for the left wall in the *Ri* 10 case, where the deviation is unacceptable high (Table 3). Also the deviation from unity of the local MTCR is limited (smaller than 14%) except at the left wall in the *Ri* 10 case (Fig. 4.). In the *Ri* 10 case the surface conditions at the left wall ($\omega = 7.21$ g/kg and $T = 20$ °C) are almost equal to the average indoor conditions, used as reference ($\omega = 7.22$ g/kg and $T = 19.5$ °C). Hence small deviations in the

Table 4
Average MTCR for the left and right wall using the inlet conditions as a reference for the Chilton–Colburn analogy (CC) and the Reynolds analogy (*Re*)

Scenario	*Ri* 0.1		*Ri* 1		*Ri* 10	
	Left	Right	Left	Right	Left	Right
Base case (CC)	1.020	1.007	1.050	1.009	1.098	1.037
Base case (*Re*)	0.857	0.846	0.883	0.849	0.931	0.879
Lewis 1 (CC)	1.016	1.031	0.996	1.018	0.991	1.017
Separate (CC)	1.015	1.012	0.988	1.066	1.469	1.548
Equal *Gr* (CC)	0.995	0.996	0.980	0.985	0.978	0.987
Uniform source (CC)	1.119	1.019	1.459	1.047	1.404	1.255
Discrete source (CC)	1.134	1.014	1.679	1.039	1.337	1.245
DiffBC1 (CC)	0.990	1.021	0.940	1.037	0.860	1.158
DiffBC2 (CC)	0.998	0.988	0.970	1.027	0.927	1.141
DiffBC3 (CC)	0.977	0.931	0.964	1.017	0.976	1.091

analogy of heat and water vapour diffusion can lead to large errors in predicted transfer coefficients. Table 4 shows that using the inlet conditions as a reference in this case reduces the deviation of the predicted average mass transfer coefficient to 10%.

In the 'Lewis 1' scenario the over or under prediction is limited to 3% for the average and for the local mass transfer coefficients except at the left wall in the *Ri* 10 case where the over prediction can be as high as 9%. As for the 'base case' scenario the left wall surface conditions lie close to the reference conditions ($\omega = 6.88$ g/kg and $T = 19.5$ °C) in the *Ri* 10 case. Using the inlet conditions as a reference reduces the error of the predicted average mass transfer coefficients to 3% (Table 4).

The deviations between the predicted and simulated mass transfer are large in the 'separate' scenario. Even if the left surface of the *Ri* 10 case is left out of the analysis deviations up to 81% are found for the average mass transfer coefficients (Table 3) and overpredictions with a factor 2–3 can be noticed for local mass transfer (Fig. 4.). The poor performance of the analogy for this latter scenario is due to the different flow regimes in the separate heat transfer case and in the separate mass transfer case: temperature differences trigger much stronger buoyancy forces than concentration differences and hence different flow patterns occur in the 'separate scenario' (if $Ri = 1$, $Gr = 2.13E10$ for the heat transfer case and $Gr = 2.37E9$ for the mass transfer case). This is confirmed by considering the 'Equal *Gr*' scenario where the temperature difference in the separate heat transfer case is lowered in such a way that the Grashof numbers of the separate heat and separate mass transport cases are equal. In this case the agreement between the predicted and simulated mass transfer is excellent. Even if the surface and reference conditions are nearly equal, the error of the predicted mass transfer is smaller than 4% for the average mass transfer coefficients and 5% for the local mass transfer coefficients.

4.2. Non-analogous boundary conditions

In many practical situations the boundary conditions for heat and moisture transfer are not analogous. How this affects the accuracy of the heat and mass transfer analogy can be seen in Fig. 5 and

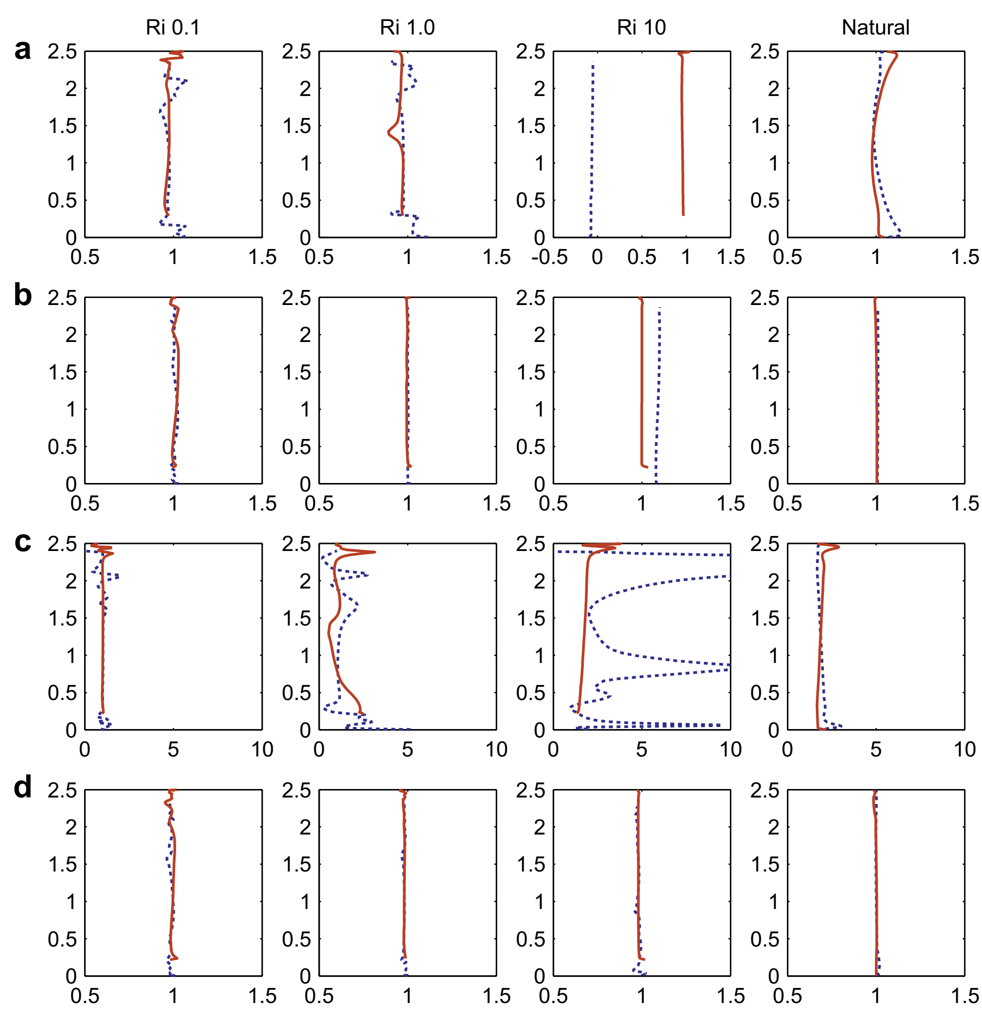

Fig. 4. Local MTCR (*x*-axis) in function of height (*y*-axis) at the left wall (------) and at the right wall (—) for (a) Base case (b) Lewis 1 (c) Separate (d) Equal *Gr*.

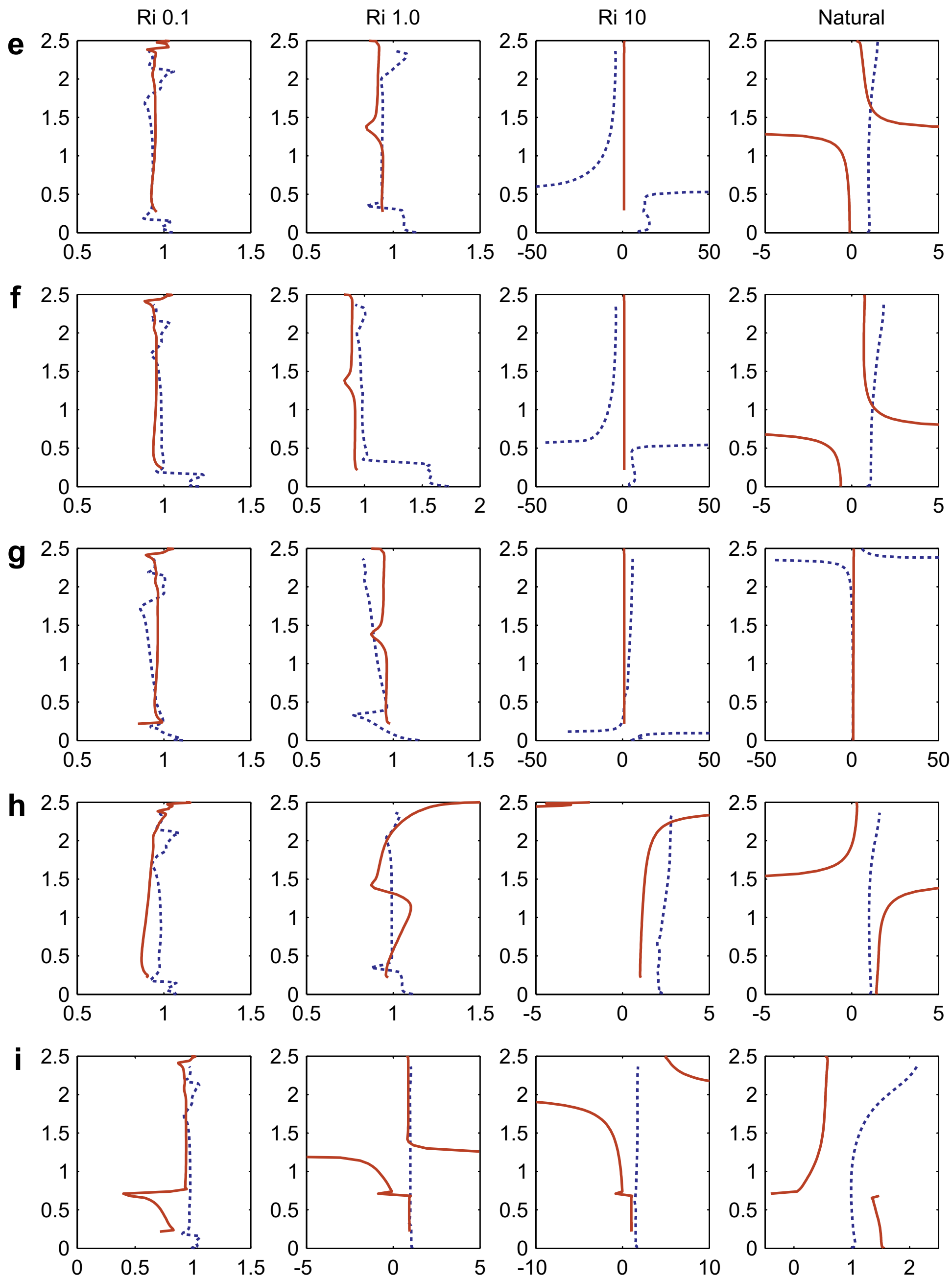

Fig. 5. Local MTCR (*x*-axis) in function of height (*y*-axis) at the left wall (– – – – – –) and at the right wall (—) for (e) Uniform Source (f) Discrete Source (g) DiffBC 1 (h) DiffBC 2 (i) DiffBC 3.

Table 3. In case of the presence of a uniform moisture source as in the 'Uniform source' scenario, the over or under prediction of the average mass transfer coefficients is smaller than 13% except for the left surface of the *Ri* 10 case and the right surface of the natural convection case. In the natural convection case the reference value for the moisture transport (ω = 13.3 g/kg) is almost equal to the value at the right surface. In the *Ri* 10 case the inlet jet sticks at the left surface (Fig. 6) hence isolating it from the bulk indoor conditions. Changes in the bulk indoor conditions will not automatically affect that surface. Errors in the predicted local mass transfer coefficients for these two cases can be as high as 5–50 times the simulated coefficients. For the other 'Uniform source' cases errors up to 15% (*Ri* 0.1 and *Ri* 1) and up to 50% (left surface of the natural convection case) are found.

In the 'Discrete source' scenario the effect on the heat and mass transfer analogy is comparable with the effect observed in the 'Uniform source' scenario, except that in the immediate neighbourhood of the source (bottom left wall) the maximum deviation between the predicted and simulated local mass transfer coefficients increases to 20% for *Ri* 0.1 and 70% for *Ri* 1.

In the first scenario with dissimilar boundary conditions (DiffBC1) deviations up to 11% are found between the predicted and simulated average mass transfer coefficients except for the left surface in the *Ri* 10 case and in the natural convection case. In these two cases the specific humidity used as reference value for mass transfer has a value of respectively 7.85 g/kg and 11.4 g/kg. These values lie in the range of the linear boundary value profile at the left surface. The reference values in the *Ri* 0.1

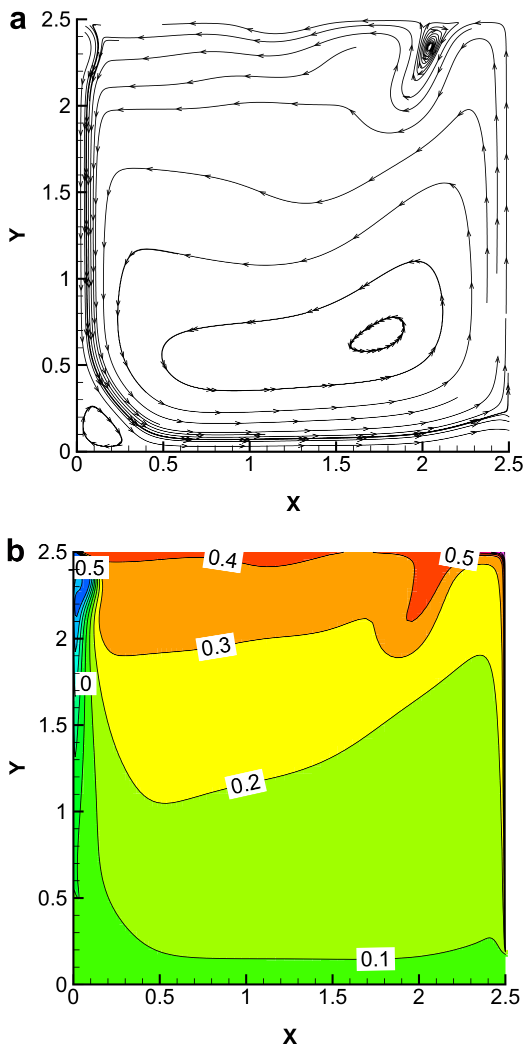

Fig. 6. Velocity vectors (a) and dimensionless specific humidity contours (b) showing that for the '*Ri*10, uniform source' case the upper left wall is isolated from the centre of the enclosure by the incoming air.

and *Ri* 1 cases lie beneath this range due to the higher ventilation rates. The local MTCR becomes zero at the position on the surface where the specific humidity is equal to the reference condition while the mass flux is different from zero. On the other hand the local MTCR attains very high positive or negative values when the local mass flux is zero while the driving force has a value different from zero. When neither the driving force nor the local flux become zero, as in the *Ri* 0.1 and *Ri* 1 cases, the effect on the local MTCR is limited to ca. 20%. In those cases a somewhat linear trend of the local MTCR in function of the specific humidity at the surface is visible.

In the 'DiffBC2' scenario the same effects are observed as in the 'DiffBC1' scenario. For the *Ri* 0.1 and *Ri* 1 cases the high ventilation rates result in an indoor specific humidity lower than the specific humidity at the wall surfaces and by consequence in driving forces and local mass fluxes different from zero. In that case the effect of the dissimilar boundary condition is limited to a more or less linear deviation from unity of the local MTCR, smaller than 20%. For the *Ri* 10 case the simulated local mass flux becomes zero for the right wall at $y = 2.4$ m which leads to extreme values of the local MTCR at that position. In the natural convection case the simulated flux is zero for the right wall at $y = 1.5$ m and the specific humidity used as reference is equal to the surface specific humidity at $y = 2$ m which leads to local MTCR reaching respectively extremely high and near zero values.

Unlike in the two previous dissimilar scenarios the mass boundary profile in the 'DiffBC3' scenario has a discontinuous course. The effect of this discontinuous profile on the predicted local mass transfer coefficients is a significant increase of the error in the vicinity of the discontinuity.

5. Discussion

5.1. Limitations of the analogy in natural convection

The very good results in the 'Lewis 1' scenario prove the capability of the heat and mass transfer analogy to accurately predict mass transfer coefficients for natural and mixed convection cases and for simultaneous heat and mass transfer. The mutual influence of heat and mass transport appears to be small in humid air, as assumed by Bottemanne [10], and does not affect the validity of the analogy. In case individual heat and mass transport problems are to be correlated extra requirements concerning the boundary conditions need to be fulfilled: comparison of the results for the 'separate' and the 'Equal *Gr*' scenario shows that the Grashof number should be equal in both the heat as the mass transfer problem. This condition is, unlike for simultaneous heat and mass transfer, not automatically fulfilled and imposes a direct relation between the temperature differences at the wall surfaces in the heat transfer problem and the species mass fraction differences in the mass transfer problem.

5.2. Chilton–Colburn or Reynolds analogy?

In practical heat and moisture transfer problems the Lewis number will be different from unity. Although it is stated in literature [4] that a Lewis factor of 1 (sc. the Reynolds analogy) can be used to model humid air, the simulations made in this paper show that this can result in an error of more than 10% on the average mass transfer coefficients. This error can easily be avoided by using the Chilton–Colburn analogy. Considering that the Lewis factor of the Chilton–Colburn analogy was originally derived for forced flows it is noteworthy that this analogy yields very good results for mixed and even natural convection flows. Simulation of local heat and mass transfer shows that the Chilton–Colburn analogy is capable of accurately predicting local mass transfer coefficients as long as the flow is attached to the surface. Fig. 7. shows that the positions at the left wall where the flow is detached for the *Ri* 0.1 case of the 'base case' scenario agree with the zone in Fig. 4. where the mass transfer is less accurately predicted.

5.3. Choice of reference condition

The major problem with the use of the heat and mass transfer analogy in indoor air flows is the correct choice of the reference condition. Due to distributions in the indoor air the conditions near the surface of interest can strongly deviate from the average indoor conditions. In case the indoor temperature and mass fraction distributions have exactly the same dimensionless profile this does not affect the analogy. Yet in practise small differences in the temperature and mass fraction distributions occur even for identical boundary and flow conditions due to variations in thermal and mass diffusivity and the mutual influence of heat and mass transfer. If the value of the chosen reference lies close to the value at the wall surface the small differences in indoor distribution can lead to extreme errors in the predicted mass transfer coefficients (eg. Table 3: left wall for *Ri* 10 case in base case scenario). In such cases the error of the predicted mass transfer coefficients can be significantly reduced by choosing a different reference condition (eg. Table 4: left wall for *Ri* 10 case in base case scenario).

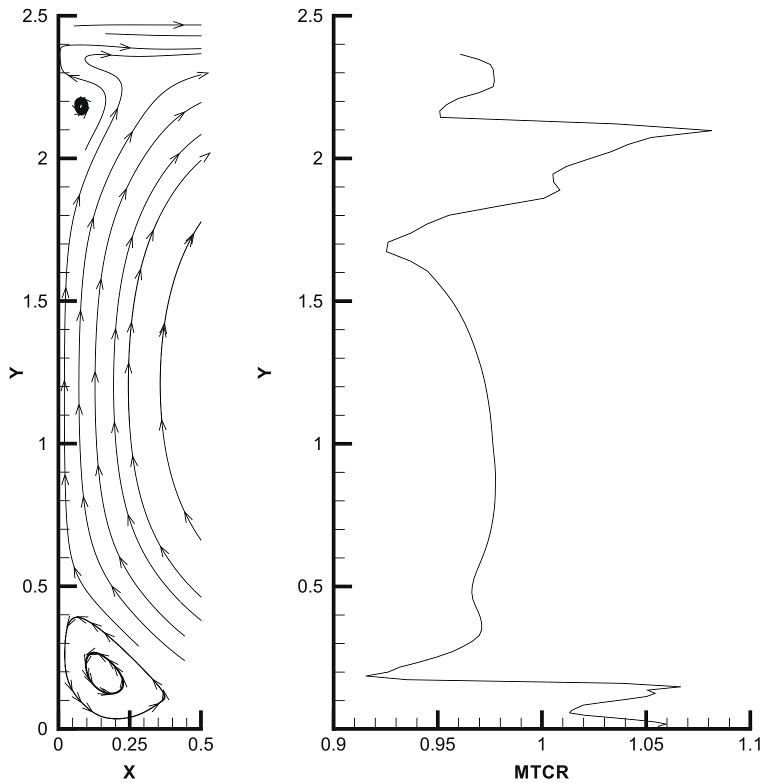

Fig. 7. Influence of the detaching flow near the left wall on the local MTCR for the '*Ri* 0.1 base case'.

Also when the boundary conditions are not similar, difficulties can arise due to the choice of the reference value. Due to different boundary conditions zero local mass fluxes can coincide with non-zero local heat fluxes. If in this case the reference condition for mass transfer differs from the surface condition, the mass transfer coefficient will become zero and the local MTCR will be extremely high (e.g. Fig. 5. right wall *Ri* 10 case of DiffBC2 scenario). The impact of this effect on the predicted average mass transfer coefficient is limited due to the integration over the entire surface (Eq. (15)). The fundamental problem with dissimilar boundary conditions is that the analogy between the indoor temperature and mass fraction distribution is no longer guaranteed as can be seen in Fig. 8. Hence in case the chosen reference is not directly linked to the wall fluxes, the analogy between the heat transfer coefficient and the mass transfer coefficient is lost. This can be seen in Fig. 5 and Table 3 for the *Ri* 10 case with uniform source.

It is thus extremely important that a direct link exists between the fluxes to the surface and the chosen reference. In this paper the mass averaged indoor conditions were used as a reference and it was found that this choice leads to good results for the prediction of the average wall flux, except for the wall covered by the falling jet in the *Ri* 10 scenario. For that wall the inlet condition is a better reference. Yet the use of the inlet condition as reference is limited as the effect of heat or moisture sources on the transfer to the other walls is not correctly taken into account.

5.4. Influence of dissimilar boundary conditions

For the studied cases with dissimilar boundary conditions where there is no problem with the chosen reference (no asymptotic behaviour in Fig. 5.) the error on the predicted average mass transfer coefficient stays limited to ca. 7% for mixed convection and ca. 40% for natural convection (Table 3). The error on predicted local mass transfer coefficients can be as high as 50% for mixed convection and up to a factor 2 for the natural convection case. The reason for these deviations is that indoor distributions, and by consequence the local transfer coefficients related to a single reference condition, are influenced by the surface conditions. The local heat transfer coefficient depends on the temperature distribution at the surface and can not be exactly related to a local mass transfer coefficient under different surface conditions. The error induced by dissimilar boundary conditions is more important for natural convection, because in natural convection the effect of the surface conditions on the indoor distribution is far greater than in flows dominated by forced convection.

5.5. Applicability of the heat and mass transfer analogy for indoor air flows

The accuracy of the heat and mass transfer analogy for the prediction of local indoor mass transfer coefficients is only guaranteed in case of perfectly similar boundary conditions and a reference sufficiently different from the surface conditions. In indoor airflows these conditions are hardly ever met due to the presence of heating systems, solar gains, heat and moisture sources, etc. It is hence recommended not to use the heat and mass transfer analogy for the prediction of local mass transfer inside buildings.

When the interest lies in predicting average mass flow rates to the walls, as in models which predict (de)humidification loads or average indoor climate, the heat and mass transfer analogy performs much better for cases with dissimilar boundary conditions. Yet the error of the predicted average mass flow rate is still very large in case the reference condition is almost equal to the surface condition or in case the average flux is not directly linked to the reference condition. In case of a transient problem it is expected that the reference and surface conditions are only equal for short

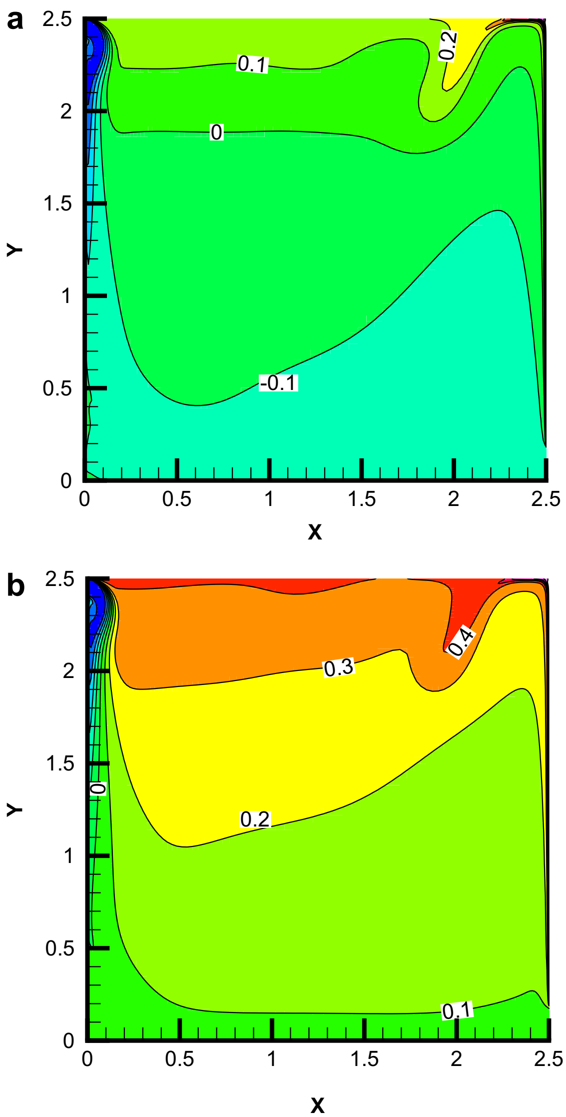

Fig. 8. Difference between the dimensionless temperature profile a) and dimensionless specific humidity profile b) for the '*Ri* 10, uniform source' case.

periods of time. Using a time averaged transfer coefficient would then yield accurate results (e.g. [17]). In case of steady-state problems it is eminent that the difference between reference and surface conditions is large enough.

It is not always possible to choose a reference which is linked to the fluxes to all the walls but in most cases the average indoor conditions can be used to predict average flow rates. The advantage of this choice is that the average indoor condition is the typical reference in the multizone simulation tools that are commonly used to predict indoor air quality or (de)humidification loads. In case of absence of heat and moisture sources the inlet conditions are a better reference, yet these cases are rather scarce.

6. Conclusions

In this paper a CFD study on the accuracy of the heat and mass transfer analogy for indoor air flows is conducted. The Reynolds and Chilton–Colburn analogy are employed for natural and mixed convection in a 2D enclosure. If the limiting conditions (Lewis number one, analogous boundary conditions, no sources) are fulfilled the analogy yields very good results for the case of simultaneous heat and mass transfer. In case of separate heat and mass transport the analogy only performs well if the Grashof number is equal in both problems. These results confirm the theoretic applicability of the heat and mass transfer analogy for indoor air flows. When the Chilton–Colburn and the Reynolds analogy are compared for cases with Lewis number different from unity the performance of the Chilton–Colburn analogy is superior.

The studied cases show that when using the heat and mass transfer analogy in indoor air flows, problems can arise due to the choice of the reference condition. In many applications one single reference is chosen to calculate the transfer coefficient at the different positions. It is however not always possible to relate all the local fluxes to a single reference. As a result it can occur that the difference between the reference condition and the surface condition is nearly zero while a non-zero local flux exists. In that case a different reference has to be chosen for the analogy to yield good results. For the cases studied in this paper the mass averaged indoor condition proved to be a good reference for most situations.

In practical cases the condition that all boundary conditions for heat and mass transfer inside buildings should be analogous is rarely fulfilled. This study shows that if the boundary conditions are not analogous, the accurate prediction of local mass fluxes using the analogy is no longer guaranteed when one single reference value is used. The prediction of average mass flow rates using one single reference is less sensitive to dissimilarities in the boundary conditions.

It is hence not recommended to use the analogy for the prediction of local mass transfer when not all restrictive conditions are met. The test cases studied in this paper indicate that the accuracy of the predicted average transfer coefficient remains good under the condition that the reference and surface conditions sufficiently differ. In that case the heat and mass transfer analogy could be used for the prediction of average transfer coefficients for problems which are not very sensitive to small variations of the transfer coefficients (e.g. prediction of (de)humidification loads or average indoor climate).

Acknowledgement

The results presented in this paper have been obtained within the frame of the FWO project B/05836/02 funded by the FWO-Flanders (Research Fund Flanders). This financial support is gratefully acknowledged.

References

[1] C.J. Simonson, M. Salonvaara, T. Ojanen, The effect of structures on indoor humidity - possibility to improve comfort and perceived air quality, Indoor Air 12 (4) (2002) 243–251.
[2] H.M. Kunzel, A. Holm, D. Zirkelbach, A.N. Karagiozis, Simulation of indoor temperature and humidity conditions including hygrothermal interactions with the building envelope, Solar Energy 78 (4) (2005) 554–561.
[3] A. Karagiozis, M. Salonvaara, Hygrothermal system-performance of a whole building, Building and Environment 36 (6) (2001) 779–787.
[4] EN15026: Hygrothermal performance of building components and building elements – Assessment of moisture transfer by numerical simulation.
[5] A. Kaya, O. Aydin, I. Dincer, Numerical modeling of heat and mass transfer during forced convection drying of rectangular moist objects, International Journal of Heat and Mass Transfer 49 (17–18) (2006) 3094–3103.
[6] A.P. Colburn, A method of correlating forced convection heat transfer data and a comparison with fluid friction, Transactions of the American Institute of Chemical Engineers 29 (1933) 174–210.
[7] J. Welty, C. Wicks, R. Wilson, G. Rorrer, Fundamentals of Momentum, Heat and Mass transfer, fourth ed., John Wiley & Sons, New York, 2001.
[8] T.H. Chilton, A.P. Colburn, Mass transfer (absorption) coefficients prediction from data on heat transfer and fluid friction, Industrial and Engineering Chemistry 26 (1934) 1183–1187.
[9] J.S. Lewis, Heat transfer predictions drom mass transfer measurements around a single cylinder in cross flow, International Journal of Heat and Mass Transfer 14 (1971) 325–329.
[10] F.A. Bottemanne, Experimental Results of Pure and Simultaneous Heat and Mass-Transfer by Free Convection About a Vertical Cylinder for $Pr = 0.71$ and $Sc = 0.63$, Applied Scientific Research 25 (5) (1972) 372–382.
[11] C.H. Bedingfield, T.B. Drew, Analogy between heat transfer and mass transfer: a psychometric study, Industrial and Engineering Chemistry 42 (6) (1950) 1164–1173.

[12] A.J.N. Khalifa, Heat Transfer Processes in Buildings, Ph.D. Thesis, University of Wales College of Cardiff, Cardiff, 1989.
[13] H.B. Awbi, Calculation of convective heat transfer coefficients of room surfaces for natural convection, Energy and Buildings 28 (2) (1998) 219–227.
[14] W. Masmoudi, M. Prat, Heat and mass-transfer between a porous-medium and a parallel external flow – application to drying of capillary porous materials, International Journal of Heat and Mass Transfer 34 (8) (1991) 1975–1989.
[15] Y.S. Tian, T.G. Karayiannis, Low turbulence natural convection in an air cavity filled square cavity – Part I: the thermal and fluid flow fields, International Journal of Heat and Mass Transfer 43 (6) (2000) 849–866.
[16] C. Beghein, F. Penot, S. Mergui, F. Allard, Numerical and experimental evaluation of turbulent models for natural convection simulation in a thermally driven square cavity, in: ASME Conference WA/HT-46, 1993, pp. 1–12.
[17] H.-J. Steeman, A. Janssens, J. Carmeliet, M. De Paepe, Modelling indoor air and hygrothermal wall interaction in building simulation: comparison between CFD and a well-mixed zonal model, Building and Environment, in press 10.1016/j.buildenv.2008.05.002.